Lasers and fiber optics[1)]

E. M. Dianov and A. M. Prokhorov

Institute of General Physics, Academy of Sciences of the USSR

Usp. Fiz. Nauk **148**, 289–311 (February 1986)

The advent of the laser and its extensive application have led to the creation of new topics in science and technology. One is modern fiber optics. The most highly developed application of fiber optics at present is fiber-optic communication. This review discusses different types and technologies of low-loss glass optical fiber, the theory of optical fibers, and certain phenomena that accompany the propagation of optical radiation in such fibers, including nonlinear optical phenomena.

TABLE OF CONTENTS

1. INTRODUCTION

The advent of the laser and its extensive application have led to the appearance of a number of new topics in science and technology. One of them is modern fiber optics, based on the low-loss glass optical fiber. Fiber-optics communication is at present the most important and developed application of fiber optics.

Low-loss glass optical fibers were developed in response to the need for a transmission medium for optical communication systems. The successful experiments of A. S. Popov were followed by the rapid development of radio communication, partly because the exploitation of the then new radio-frequency range was accompanied by the development of monochromatic sources of radio-frequency waves. It was well understood that a larger amount of information could be transmitted by reducing the wavelength of these waves. The optical range remained practically unused for communication purposes, mostly because monochromatic sources of radiation were not available in optics. However, the advent of the laser led to the development of communication lines for the optical band. The initial infrastructure was thus made available, and all the necessary ideas had already been developed in the radio-frequency band. Early experiments on the transmission of information through the free atmosphere by means of the laser beam showed that the atmosphere was not a suitable medium for the transmission of light to large distances because of meteorological factors. The effects of atmospheric instabilities on the light beam could be removed by pipes incorporating correcting components, but this meant that the transmission lines became complex, large, and expensive.

Glass optical fibers had been used even prior to the invention of the laser, but their loss exceeded 1000 dB/km, and it was considered that they were not promising for communication purposes. In 1966, Kao and Hockham[1] showed that the high loss of glass optical fibers was due to impurities present in glass, and that a figure of less than 20 dB/km could be achieved in the optical range. This work was a powerful stimulus to the development of low-loss optical fibers. In 1970, the Corning Glass Company in the United States produced optical glass fibers with a loss of less than 20 dB/km in the visible range. In the same year, Zh. I. Alferov *et al.* succeeded in producing continuous generation at room temperature in a semiconductor laser based on the GaAlAs double heterostructure.[2] These two advances provided the basis for the development of fiber-optic communication. In not much more than another five years, optical fibers based on high-silica glass with extremely low loss of the order of a few tenths of dB/km ($\sim 10^6$ cm^{-1}) in the near infrared were developed. The availability of glass optical fibers with such low optical loss in turn stimulated intensive development work on other optical communication systems, including long-life (in excess of 10^5 h) semiconductor lasers, photodetectors, components for integrated optics, and so on. This led to rapid advances in fiber-optic communication.

Many different fiber-optic communication systems have been tested in many countries under practical conditions during the last ten years. At present, the most extensive application of optical fiber communication is in the telephone network. Low-loss optical fibers are also very promising for cable television, and major projects involving the setting up of fiber-optic cable television have been established in all developed countries. In particular, in May 1984, practical tests began in Moscow on the first optical-fiber cable TV line supplying television signals to a house on Ural'skaya Street, which is in an area with poor television reception. These trials demonstrated the technological and economic

 0038-5670/86/020166-13$01.80

utility of these systems. World wide, low-loss optical fibers are now being manufactured at the rate of about 10^6 km/y.

Fiber-optic cables have obvious advantages as compared with coaxial cables. They have no need for scarce nonferrous metals (copper, lead, and so on) and are highly immune interference. Their most important advantage is that they can transmit information at high speed to large distances without repeaters. For example, fiber-optic communication systems have now been developed for data transmission at the rate of 4 Gbit/s to distances in excess of 100 km without repeaters.[3] The enormous possibilities of fiber-optic communication and the present state of development of the necessary infrastructure is illustrated by the underwater fiber-optic communication cables that are at present being installed under the Atlantic and Pacific Oceans.

Recent years have seen a number of new applications of the low-loss glass optical fiber. These include optic-fiber sensors for different physical fields (acoustic waves, temperature, magnetic waves, rotation, and so on) in which the optic fiber is the sensitive element,[4] and also the use of optic fibers for the channeling of powerful laser radiation for medical and technological purposes.[5]

Nonlinear fiber optics is a further important and interesting application.[6] High-silica glass is not highly nonlinear, but the very considerable length of low-loss optic fibers and their small cross section have sharply reduced the threshold for different nonlinear phenomena. This has also substantially extended the range of possible experiments because it is now possible to use as pump sources the relatively low-power tunable dye and doped-crystal lasers.

All this has been responsible for the extensive interest in nonlinear fiber optics, and very interesting results have been reported in recent years. They include the observation of the soliton mode of propagation of optical pulses, the production of the femtosecond optical pulses, the development of the soliton laser, and so on. Nonlinear optical communication lines are under discussion in the literature.[47-56]

In this review, we shall consider the types and technology of low-loss optical fibers, the theory of optical fibers, and some phenomena accompanying the propagation of optical radiation along a fiber.

At the end, we shall consider possible future development of fiber optics.

2. TYPES OF OPTICAL FIBER AND FABRICATION TECHNOLOGY

The typical optical fiber is a long filament with a diameter of 100–1000 μm, depending on the particular application. It consists of a cylindrical glass core surrounded by cladding with a lower refractive index (Fig. 1). The cladding is usually made of glass, but different polymers are also used. Optic fibers can be divided into multimode and single mode fibers, depending on the number of modes that can propagate along the lightguide. The core diameter $2a$ is usually 5–8 μm for single-mode fibers working in the nearinfrared, and between a few tens and a few hundred μm in the case of multimode fibers. The difference between the refractive indices of the core and cladding, $\Delta n = n_1 - n_2$, produces the

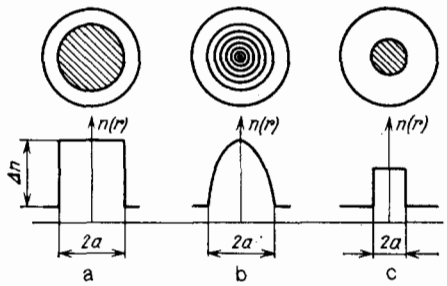

FIG. 1. Cross section and refractive index profile of multimode step-index (a), multimode graded-index (b), and single-mode fibers.

channeling of light by total internal reflection at the core-cladding separation boundary, and is usually 1–2% for multimode fibers and a few tenths of a per cent for single-mode fibers. The numerical aperture

$$NA = (n_1^2 - n_2^2)^{1/2} = \sin\theta_c,$$

is an important parameter of the optic fiber, where θ_c is the maximum angle between the light ray and the fiber axis for which propagation as a result of total internal reflection is still taking place.

Three basic types of optical fiber are manufactured at present, depending on application (see Fig. 1).

1. Step-index multimode fibers with high numerical aperture (0.29–0.30) and a large core diameter (a few hundred μm). This class of fiber has been developed for low rates of data transmission (tens or hundreds of Mbit/s) over short distances.

2. Graded-index multimode optic fibers for wide-band long-distance communication lines. Here the data transmission rate is up to 140 Mbit/s or higher, and the distances are 20–40 km. As a rule, the core diameter of these fibers is 50 μm, the total diameter is 125 μm, and the numerical aperture is 0.20–0.23.

3. Single-mode optic fibers for data transmission rates in excess of 140 Mbit/s and distances in excess of 40 km. These are also widely used in fiber-optic sensors of different physical fields.

The greatest advances have now been achieved in the development of optic fibers based on high-silica glass. These fibers have the lowest loss (fraction of dB/km in the near infrared) and the greatest mechanical strength (up to 5 GPa). The core and cladding material is usually high-silica glass doped with GeO_2, P_2O_5, B_2O_3, or F^-. These dopants are essential if the necessary optical and thermophysical parameters of the core and cladding material (refractive index, softening point, etc.) are to be achieved. F^- and B_2O_3 reduce the refractive index of the high-silica glass, whilst all other dopants tend to increase it. Any dopant will reduce the melting point of high-silica glass.

The fabrication technology used for fibers of this kind is based on the chemical deposition of fiber material from the vapor phase, the initial materials being volatile halides and oxygen. The volatile halides are usually the chlorides of silicon, germanium, and boron, phosphorus oxychloride, and

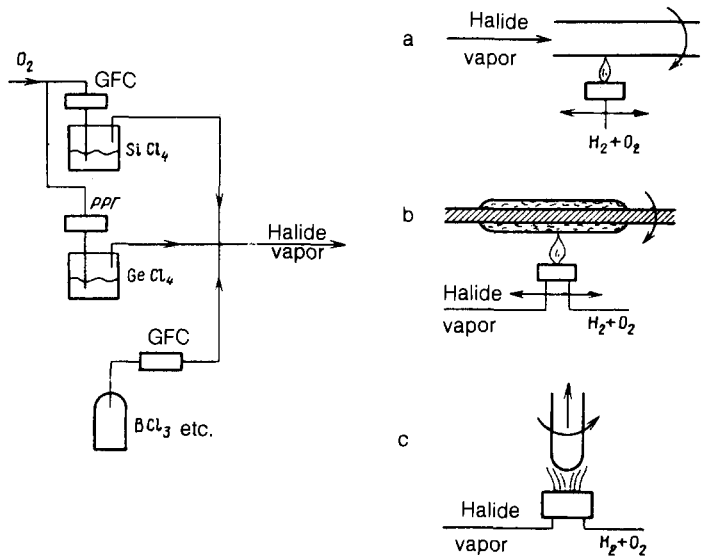

FIG. 2. Diagram illustrating the fabrication of optical-fiber preforms by chemical deposition from the vapor phase: a—inside process (MCVD), b—outside process (OVD), c—axial deposition (VAD).

boron bromide. The principle of fabrication of the fiber preform by chemical deposition from the vapor phase is illustrated schematically in Fig. 2. The left-hand side of the figure shows the scheme used to produce the halide vapor. Oxygen is used as the carrier gas. The gas flow controllers (GFC) are used to vary the supply of the compounds necessary to produce the preform.

Three methods are used in commercial fabrication of high-silica optic fibers. In the first method (Fig. 2a), which is frequently referred to as the inside deposition process, the reaction between the halide vapor and oxygen occurs inside a rotating fused-silica tube (substrate tube). This produces fine particles of silicon dioxide and of the dopants, which are deposited on the inner surface of the substrate tube. The resulting layer of porous glass is then fused into bubble-free transparent glass by a gas torch moving along the tube. This procedure produces layer after layer of the cladding, and then the core. When a sufficient number of such layers has been deposited, the temperature is raised and the tube collapses into the preform rod. The preform has the necessary internal waveguide structure (core surrounded by the lower-index cladding), and is ready for drawing out into a fiber.

In the second method (Fig. 2b), called the outside deposition process, the halides are oxidized in the flame of the torch, and the resulting fine oxide particles are deposited on the outer surface of a rotating cylindrical substrate (bait rod), with the gas burner moving along the rod. This produces the porous material of the core and then of the cladding. The porous preform is then slipped off the bait rod and is zone-sintered and simultaneously dried. The collapse of the transparent preform and the drawing out into the fiber is performed in a single technological operation.

In the third method (Fig. 2c), called the vapor phase axial deposition process, the porous material is deposited on the end of a rotating fused-silica bait rod. The resulting porous preform is again zone-sintered and simultaneously dried.

All three methods can now be used to produce fibers of comparable quality. However, their productivities are different. A single preform produced by the internal deposition method can be used to draw out ~ 10 km of fiber (125 μm diameter), whereas the preform produced by the outside method will produce several tens of km. The axial deposition method produces preforms from which 100 km of fiber can be drawn and, in principle, is capable of continuous production of optic fiber.

The next operation in lightguide fabrication is to draw the fiber from the preform, with the simultaneous deposition of a polymer coating.

In principle, the drawing process is simple (Fig. 3). The preform is fed by a precision preform drive mechanism into a furnace in which the tip of the preform is melted. The optic fiber, retaining the waveguide structure of the preform, is drawn from this molten glass at a rate of a few tens of m/min and up to 60 m/min. The drawing of high-silica fiber waveguides is not a simple task because the temperature in the hot zone of the furnace must be 2200 °C. At present, the preform is usually heated in a graphite resistance furnace, an induction furnace, or an oxyhydrogen torch. A promising alternative approach is to use the CO_2-laser (see, for example, Ref. 7).

The drawing process has an important influence on the parameters of optic fibers, especially their mechanical strength. This strength must be sufficient to withstand the applied load when the fiber-optic cable is manufactured, installed, and used.

The theoretical strength of glass, which is determined by atomic bonding forces, is very high. Estimates show that the breaking point is about 20 GPa. Figures of up to 16 GPa have been recorded in many experiments. However, most glass components have much lower strength, usually 30–100 MPa. Moreover, it has been noted that various defects (inhomogeneities, inclusions, cracks) give rise to a substantial reduction in the strength of glass and, as a rule, the strength of glass samples is determined by surface defects.

The lower strength of glass as compared with the theo-

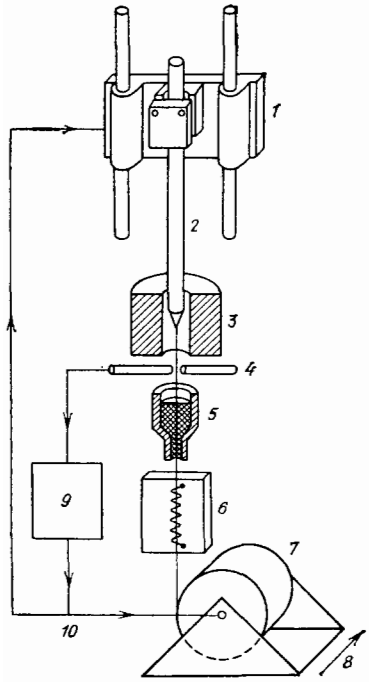

FIG. 3. Schematic of fiber-drawing machine used to produce optical fibers from preforms: 1—precision preform drive mechanism, 2—preform, 3—furnace, 4—fiber diameter sensor, 5—deposition of primary coating on fiber, 6—furnace for the polymerization of primary coating, 7—precision takeup drum, 8—displacement of drum for layered winding, 9—fiber diameter control feedback system, 10—preform drive mechanism control or takeup-drum control.

retical value is explained by the Griffiths microcrack hypothesis. In this model, it is postulated that very small cracks are present on the surface of the glass sample. The tensile stress applied to the sample is concentrated at the tip of the crack, the local stress may become equal to the theoretical stress of the glass, and the atomic bonds are broken. However, the *average* stress in the sample can still be quite low. This approach leads to a fracture criterion for glass in the form $\sigma^{1/2}(a) = \text{const}$ where σ is the applied stress and a is the semi-major axis of the crack, assumed to be elliptic in cross section.[8]

Estimates show that the presence of a crack with $a = 0.03\ \mu$m in the glass fiber will lead to fracture under a tensile load of 3.5×10^3 MPa.

The validity of the Griffiths hypothesis has been confirmed by the many successful applications of methods of increasing the strength of glass based upon it. They include ion exchange, chemical etching, and so on. The hypothesis has also been confirmed by the fact that the strength of freshly fabricated glass fibers is greater by several orders of magnitude than the strength of fibers left unprotected for several days in the laboratory.

A glass sample contains many cracks, but it is the largest crack that is responsible for the fracture of the sample under stress. There is no way at present of determining the size and position of the largest crack in a sample and, since each specimen has in general a crack size distribution, it is clear that the strength of glass is an essentially statistical parameter. Measurements of strength are usually analyzed in terms of Weibull statistics, based on the weakest-link model. The probability that a fiber of length l will fail when a tensile stress σ is applied to it is satisfactorily described by the Weibull probability formula

$$F(\sigma, l) = 1 - \exp\left[\frac{l}{l_0}\left(\frac{\sigma}{\sigma_0}\right)^m\right]$$

or $\ln\ln[1/(1-F)] = m \ln(\sigma/\sigma_0) + \ln(l/l_0)$ where F is the fraction of fiber samples of length l that fail under a given load and l_0, σ_0, m are constants, determined by failure testing of a large number of samples.

The quantity m is inversely proportional to the spread in the strength of samples. For optic fibers with a small spread in their longitudinal strength, the Weibull distribution has a steep slope (m is large).

Numerous studies of the failure of glass optic fibers and of the effects of fabrication technology on their strength have been carried out in the course of the last decade (see, for example, Refs. 9–12) and have led to the development of light fibers with tensile strengths of up to a few GPa for fiber lengths of the order of 10 km. These studies have demonstrated that high-strength optic fibers must satisfy the following basic conditions:

1. High optical quality of the substrate tube. Synthetic high-silica glass is preferred.

2. The preform must have a high-quality surface. The preform must be etched or fired, or both, prior to the drawing process.

3. The preform must be heated under sterile conditions during the drawing process. The heating of the preform with a CO_2 laser beam seems to be promising.

4. The deposition of polymer coatings during the drawing process must not damage the surface of the optic fibers.

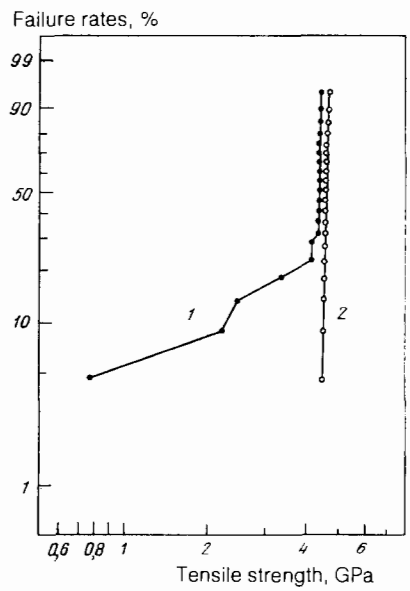

FIG. 4. Failure probability distribution for synthetic high-silica fibers. Sample length 20 m, number of samples 20. 1—standard atmosphere in graphite furnace, 2—dust free atmosphere in furnace.

The most common materials for covering the optic fiber during the drawing process are epoxy resin curved by ultraviolet radiation, or silicone rubber vulcanized at moderate temperatures. The thickness of the coating ranges from a few μm to several tens of μm.

Figure 4 shows the Weibull distribution describing the probability of failure for synthetic high-silica glass fibers drawn with the aid of a graphite furnace.[11] Dust particles in the furnace have a very considerable effect on the strength of the fibers.

3. THEORY OF PROPAGATION OF OPTICAL RADIATION IN REGULAR OPTIC FIBERS

Ray theory describes correctly the basic features of propagation of light in an optic fiber, but more detailed information can only be obtained by solving Maxwell's equations. The theory of regular optic fibers is now in a satisfactory state and is described in great detail in the literature (see, for example, Refs. 13–15), so that we shall confine our attention to a brief presentation of the method of solution and of the final results for some simple cases.

Maxwell's equations can be reduced to the scalar wave equation

$$\nabla^2\psi = \varepsilon\mu \frac{\partial^2\psi}{\partial t^2}, \tag{1}$$

where ψ represents each of the components of **E** and **H**, and ε and μ are the permittivity and magnetic permeability, respectively. Equation (1) is valid on the assumption that ε is constant in space. Marcuse[13] has shown that the wave equation (1) is approximately valid wherever the variation in ε is small over distances of the order of one wavelength. This is precisely what happens in an optic fiber.

Consider a cylindrical set of coordinates ρ, φ, z, such that the z axis lies along the axis of the fiber, and assume that the permittivity is independent of z. The transverse field components E_ρ, E_φ, H_ρ, and H_φ can be expressed in terms of E_z and H_z by using the Maxwell equations written in terms of cylindrical coordinates.

We shall seek the solutions in the form

$$\begin{aligned} E &= E(\rho, \varphi)\exp[-i(\omega t - \beta z)], \\ H &= H(\rho, \varphi)\exp[-i(\omega t - \beta z)], \end{aligned} \tag{2}$$

where β is the longitudinal propagation constant. The transverse field components are then given by

$$\left.\begin{aligned} E_\rho &= -\frac{i}{\varkappa^2}\left(\beta\frac{\partial E_z}{\partial\rho} + \frac{\mu\omega}{\rho}\frac{\partial H_z}{\partial\varphi}\right), \\ E_\varphi &= -\frac{i}{\varkappa^2}\left(\frac{\beta}{\rho}\frac{\partial E_z}{\partial\varphi} - \mu\omega\frac{\partial H_z}{\partial\rho}\right), \\ H_\rho &= -\frac{i}{\varkappa^2}\left(\beta\frac{\partial H_z}{\partial\varphi} - \frac{\omega\varepsilon}{\rho}\frac{\partial E_z}{\partial\varphi}\right), \\ H_\varphi &= -\frac{i}{\varkappa^2}\left(\frac{\beta}{\rho}\frac{\partial H_z}{\partial\varphi} + \omega\varepsilon\frac{\partial E_z}{\partial\rho}\right), \end{aligned}\right\} \tag{3}$$

where

$$\varkappa^2 = k^2 - \beta^2 = \left(\frac{2\pi n}{\lambda}\right)^2 - \beta^2, \tag{4}$$

and k is the propagation constant in a medium of refractive index n.

The components E_z and H_z can be found by solving the scalar wave equation (1) in cylindrical coordinates. These equations are rigorous for E_z and H_z because ε is independent of z.

Separation of variables is achieved by taking the solutions in the form

$$\begin{aligned} E_z &= AF(\rho)\, e^{i\nu\varphi}, \\ H_z &= BF(\rho)\, e^{i\nu\varphi}. \end{aligned} \tag{5}$$

The differential equation with respect to φ shows that the constant ν must be an integer in order to ensure azimuthal periodicity. The differential equation for $F(\rho)$ is

$$\frac{\partial^2 F}{\partial\rho^2} + \frac{1}{\rho}\frac{\partial F}{\partial\rho} + \left(k^2 - \beta^2 - \frac{\nu^2}{\rho^2}\right)F = 0. \tag{6}$$

So far, we have not defined the structure of the optic fiber. However, we must now consider this structure because the solutions for β and $F(\rho)$ are found from (6) by imposing the appropriate boundary conditions. The simplest structure of an optical fiber for which (6) can be solved is the step-index structure. The fiber then consists of a uniform core of diameter $2a$ and refractive index n_1, and a surrounding infinite cladding of refractive index n_2. Physical considerations immediately show that the solutions must satisfy the following conditions: $F(\rho)$ finite for $\rho = 0$, and $F(\rho)\to 0$ for $\rho\to\infty$.

For $\rho < a$, these conditions are satisfied by the Bessel function J_ν, so that

$$\begin{aligned} E_z &= AJ_\nu(u\rho)\, e^{i\nu\varphi}, \\ H_z &= BJ_\nu(u\rho)\, e^{i\nu\varphi}, \end{aligned} \tag{7}$$

where $u^2 = k_1^2 - \beta^2$, $k_1 = 2\pi n_1/\lambda$, and A, B are constants.

For $\rho > a$, the above conditions are satisfied by the modified Hankel functions, and the solution has the form

$$\begin{aligned} E_z &= CK_\nu(w\rho)\, e^{i\nu\varphi}, \\ H_z &= DK_\nu(w\rho)\, e^{i\nu\varphi}, \end{aligned} \tag{8}$$

where $w^2 = \beta^2 - k_2^2$, $k_2 = 2\pi n_2/\lambda$, and C, D are constants.

The quantity $V = (u^2 + w^2)^{1/2} a = (2\pi a/\lambda)(n_1^2 - n_2^2)^{1/2}$ is the characteristic parameter (or normalized frequency) of the fiber and, as we shall see later, it contains a lot of information about the fiber properties.

We must now analyze (7) and (8). As $w\rho\to\infty$, we have $K_\nu(w\rho)\to e^{-w\rho}$. Physical considerations show directly that $w > 0$ for $\rho\to\infty$. Consequently, $\beta \geqslant k_2$. The equality sign gives the cut-off condition, in which case $w = 0$ and the field leaves the fiber. Inside the core, the constant u must be real, so that $k_1 > \beta$. The propagation constant is thus seen to have the following range of allowed values:

$$k_2 \leqslant \beta \leqslant k_1. \tag{9}$$

The exact solution for β is found from the conditions of continuity of the tangential components of the fields $\bar{E}$ and $\bar{H}$ across the boundary $\rho = a$. These conditions give a set of four homogeneous equations for the unknowns A, B, C, and D. The equation for the eigenvalues β (the characteristic equation) is obtained by setting the determinant of this system equal to zero:

$$\left[\frac{J_\nu'(ua)}{uJ_\nu(ua)}+\frac{K_\nu'(wa)}{wK_\nu(wa)}\right]\left[\frac{k_1^2J_\nu'(ua)}{uJ_\nu(ua)}+\frac{k_2^2K_\nu'(wa)}{wK_\nu(wa)}\right]$$
$$=\nu^2\beta^2\left(\frac{1}{u^2}+\frac{1}{w^2}\right),$$
$$\beta=\frac{2\pi a}{\lambda}\left(\frac{n_2^2u^2+n_1^2w^2}{u^2+w^2}\right)^{1/2}. \qquad (10)$$

The primes in this equation represent differentiation with respect to the complete argument. This equation allows only discrete values of β within the range defined by (9).

For $\nu=0$, the solution consists of transverse magnetic ($H_z=0$) and transverse electric ($E_z=0$) modes (*TM* and *TE*, respectively) in the conducting hollow cylinder.

When $\nu\neq0$, we have the hybrid modes $HE_{\nu m}$ and $EH_{\nu m}$. Both E_z and H_z of these modes are nonzero. The designations *HE* and *EH* depend on which of the components (E_z or H_z) gives the greater contribution to the transverse field.

The oscillating character of the Bessel function $J_\nu(u\rho)$ means that equation (10) has m roots for a given ν.

An important mode parameter is its cut-off frequency which corresponds to $w=0$ and, consequently, $V=u_m a$. The cut-off conditions corresponding to different modes are given by the following equations:

$$\left.\begin{aligned}&\mathrm{EH}_{\nu m},\mathrm{HE}_{1m}: && J_\nu(u_m a)=0,\\ &\mathrm{HE}_{\nu m}: && (n_1^2+1)\,J_{\nu-1}(u_m a)=\frac{u_m a}{\nu-1}J_\nu(u_m a),\\ & && \nu=2,\ 3,\ 4,\ \ldots,\\ &\mathrm{TE}_{0m},\ \mathrm{TM}_{0m}: && J_0(u_m a)=0.\end{aligned}\right\} \qquad (11)$$

The only mode with zero cut-off frequency is HE_{11}. By choosing the fiber parameters (a, Δn) for given wavelength so that the next higher modes TE_{01}, TM_{01}, and HE_{21}, which have higher cut-off frequencies, cannot propagate, we can determine the conditions for the propagation of the mode HE_{11}, i.e., the optic fiber is then a single-mode fiber. This occurs when $V=2\pi a/\lambda)\,(n_1^2-n_2^2)^{1/2}<2.405$. Figure 5 shows a graph of the propagation constant β/k_0 for a number of low-order modes.

Let us now consider the power distribution in a given mode within the core and cladding. This distribution is obtained by integrating the Poynting vector over each part of the fiber cross section. Marcuse[13] has shown that the power propagating in the cladding in a region well away from the cut-off is given by

$$\frac{P_{\mathrm{cla}}}{P_\Sigma}=\left[\frac{u_m^\infty a}{V}\right]^4\left(1-\frac{2}{V}\right), \qquad (12)$$

where u_m^∞ is the mth root of the equation $J_\nu(u_m^\infty a)=0$. It is clear that

$$\frac{P_{\mathrm{core}}}{P_\Sigma}=1-\frac{P_{\mathrm{cla}}}{P_\Sigma}.$$

Hence it is clear that, as V increases, the fraction of power transported by any mode in the cladding will decrease. For example, for the HE_{11} mode, about 70% of the power is transported in the cladding and 30% in the core when $V=1$, whereas for $V=2.405$, for which the next group of modes begins to propagate, approximately 84% of the power is transported in the interior of the core.

We already saw in (8) that the field distribution in the cladding behaves as $K_\nu(w\rho)$. For large values of $w\rho$, it is found that $K_\nu(w\rho)\to\exp(-w\rho)$, so that when $\rho=w^{-1}$ the field has fallen by a factor of e from its maximum value. If we take this value of ρ as the mode radius $\rho_{\nu m}$, we can show that

$$\rho_{\nu m}=\frac{1}{w}=\frac{a}{\{V^2-(u_m^\infty a)^2[\pm1-(2\nu/V)]^{1/\nu}\}^{1/2}}. \qquad (13)$$

For example, for the HE_{11} mode with $V=1$, the mode radius is $\rho_{11}\simeq3a$. Thus, the thickness of the cladding must exceed this value if perturbations of the field in the fiber are to be avoided.

It will be useful at this point to give the expression for the total number of modes propagating in a fiber with given V. It has been shown[17] that, to a good approximation, the total number of modes is given by

$$N=\frac{V^2}{2}. \qquad (14)$$

So far, we have confined our attention to an optic fiber consisting of a uniform core surrounded by infinite cladding. There is one other distribution of the refractive index over the cross section of the fiber for which an exact solution of the scalar wave equation can be obtained. This is the quadratic index variation of the form

$$n^2(\rho)=n^2(0)\left[1-2\Delta\left(\frac{\rho}{a}\right)^2\right], \qquad (15)$$

where $n(0)$ is the refractive index on the axis of the fiber. Multimode optical fibers with this refractive index profile are of major practical interest because, as we shall see later, the near-parabolic index distribution equalizes the group velocities of different modes and extends very substantially the data transmission band width as compared with the step-index fiber. The solution of this problem is given in Ref. 13 and will not be examined in detail here. We merely note that, in this case, the fields can be expressed in terms of the well-known Laguerre-Gauss functions. The mode propagation constant is given by the simple expression

$$\beta_{p,q}=n(0)\,k\left[1-\frac{2\sqrt{2}\Delta}{n(0)\,ka}(p+q+1)\right]^{1/2}. \qquad (16)$$

In view of the importance of graded-index fibers in optic-

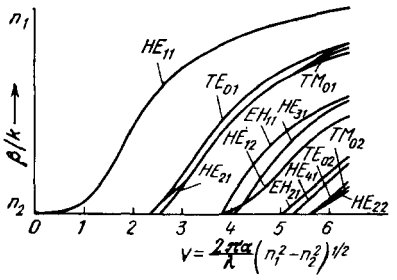

FIG. 5. Reduced propagation constant as a function of V for some of the lowest-order modes in a step-index fiber.

fiber communication systems, it is desirable to find simple solutions for optical fibers with a more general index distribution. This problem has been solved[18] by the WKB method, well known in quantum mechanics.

A substantial simplification of the problem can be achieved in the approximation of weakly-guided modes for which $n_1 \simeq n_2$. It has been found[16,17] that, when $n_1 \simeq n_2$, the $HE_{\nu+1,m}$ and $EH_{\nu-1,m}$ propagation constants are almost equal. This suggests that it may be possible to simplify the problem by taking E_z and H_z in the form of a linear combination of solutions. Having determined the transverse field components with the aid of (3), we find that (in Cartesian coordinates)

$$\left.\begin{aligned} &E_x = H_y = 0, \\ &E_y = AJ_\nu(u\rho)\begin{pmatrix}\cos\nu\varphi\\ \sin\nu\varphi\end{pmatrix}, \\ &H_x = -nA\left(\frac{\varepsilon}{\mu}\right)^{1/2} J_\nu(u\rho)\begin{pmatrix}\cos\nu\varphi\\ \sin\nu\varphi\end{pmatrix}, \end{aligned}\right\} \qquad (17)$$

where $n \simeq n_1 \simeq n_2$.

Thus, it is clear that the chosen linear combination represents a wave that is linearly polarized in the y direction. Obviously, the form of the transverse field that we have obtained is simpler than the exact solution. Similar expressions are obtained for the mode with the orthogonal polarization. Repeating the same operation for the region $\rho > a$ (with the Bessel function replaced with the modified Hankel function), it can be shown that linearly polarized fields are the only ones present.

Application of the boundary conditions leads to the following equation for the eigenvalues β:

$$\frac{uJ_{\nu\pm1}(ua)}{J_\nu(ua)} = \mp\frac{wK_{\nu\pm1}(wa)}{K_\nu(wa)}. \qquad (18)$$

This equation is clearly much simpler than (10). Snyder[16] has shown that the solution of this approximate equation gives rise to an error of not more than 1% for $\Delta = (n_2 - n_2)/n \leqslant 0.1$ and 10% for $\Delta \leqslant 0.25$.

Linearly polarized modes are designated $LP_{\nu m}$ in the literature. The lowest order mode is LP_{01}. The relationship between different mode designations is as follows:

$$\mathrm{LP}_{01} - \mathrm{HE}_{11},$$
$$\mathrm{LP}_{\nu m} - \mathrm{HE}_{\nu+1,m} \pm \mathrm{EH}_{\nu-1,m}, \mathrm{TE}_{0m}, \mathrm{TM}_{0m}.$$

4. OPTICAL PHENOMENA IN GLASS FIBERS

The propagation of optical radiation in an optical fiber is accompanied by a number of phenomena that are of both practical and scientific interest. One of them is the attenuation of the optical signal. Studies of the mechanisms responsible for the optical loss and its spectral dependence enable us not only to obtain minimum-loss optical fibers, but also to select materials and spectral intervals for particular applications of a fiber of a given material.

Another phenomenon that is important in practice is the broadening of a short optical pulse as it propagates along an optical fiber. This phenomenon is important, above all, because the broadening of a pulse restricts the rate at which data can be transmitted along the lightguide in optical communication systems. In this Section, we shall also examine nonlinear optical phenomena which have a number of important features in optical fibers.

4.1. Optical loss in glass fiber lightguides

We shall examine the origin of optical loss in glass lightguides by taking the high-silica glass lightguide as an example because this is the most widely used fiber at present and its optical loss has been extensively studied. High-silica glass has maximum transparency in the visible and near infrared parts of the spectrum. The optical loss of glass is determined by fundamental (intrinsic) absorption and scattering mechanisms, and by absorption and scattering by impurities and defects.

Additional loss due to the scattering of light by inhomogeneities in the waveguide structure is possible in optical fibers.

The fundamental mechanisms responsible for optical loss in the above spectral interval include the tails of electronic absorption bands in the ultraviolet as well as the infrared lattice absorption and scattering of light by inhomogeneities present in glass with linear dimensions smaller than the wavelength (Rayleigh scattering).

Figure 6 shows estimates of the fundamental optical loss in high-silica glass, obtained by extrapolating the electronic and phonon fundamental absorption edges to the high-transparency region, and also by taking Rayleigh scattering into account.[19] Absorption was calculated from the transmission spectra of ultrapure high-silica glass samples in the ultraviolet and near infrared, and the Rayleigh scattering curve was obtained by extrapolating the loss due to scattering, measured in highly homogeneous high-silica glass specimens at 0.63 μm, using the λ^{-4} law. It is clear from the figure that the maximum transparency region of high-silica glass lies in the range 1–1.17 μm, where the absolute minimum of optical loss occurs at 1.55 μm and amounts to about 5×10^{-7} cm^{-1} ($\sim$0.2 dB/km).

As far as impurity absorption is concerned, in the near infrared it is mostly due to transition-metal impurities such as Fe, Cu, Ni, Cr, V, and so on, and also hydroxyl groups.

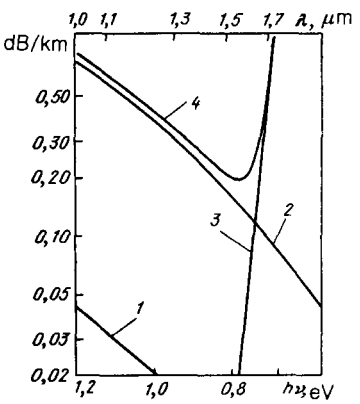

FIG. 6. Fundamental optical loss in high-silica glass, doped with germanium, as a function of wavelength and photon energy: ultraviolet absorption (1), Rayleigh scattering (2), infrared lattice absorption (3), total (4).

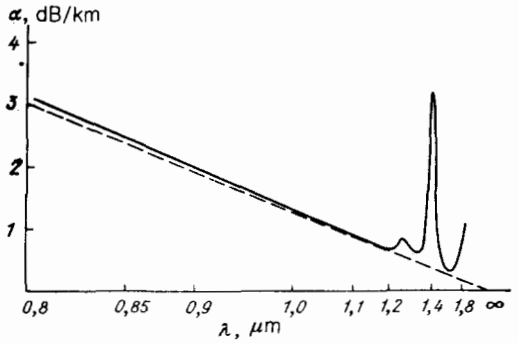

FIG. 7. Optical loss spectrum of a graded-index multimode fiber with a high-silica glass core doped with germanium dioxide. Broken line shows the theoretical limit due to Rayleigh scattering.

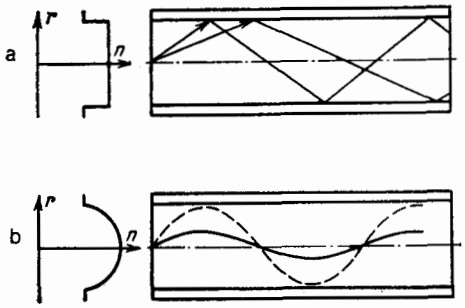

FIG. 8. Ray propagation in a step-index (a) and graded-index (b) optical fiber.

Absorption by transition-metal impurities and hydroxyl groups can be reduced to negligible levels by reducing their concentration to a few parts per billion (10^{-9}) and a few parts per million (10^{-6}), respectively. The methods developed by Devyatykh *et al.* for the removal of volatile halides can be used to produce silicon chlorides, germanium chlorides, and so on, containing metals, organic materials, and water at the level of 10^{-7}–10^{-8} mass %, 10^{-4} mol %, and 10^{-5} mol %, respectively.[20,21] This degree of purity of the initial compounds, combined with the well developed technology of fabrication of optical fibers, has resulted in improved fibers without additional contamination of glass during the fabrication process. The corresponding optical loss is close to the theoretical limit.

Figure 7 shows the optical loss spectrum of a graded-index multimode optical fiber[22] with a high-silica glass core, doped with germanium dioxide. It is clear that, with the exception of the small absorption peak near 1.38 μm, which is due to absorption by the hydroxyl groups, the optical loss is close to the theoretical limit set by Rayleigh scattering. The minimum loss at 1.5 μm amounts to 0.25 dB/km.

It follows that the most promising spectral interval for optical fiber transmission (if retranslation repeaters are not to be used) is the wavelength range 1.2–1.6 μm where optical loss in high-silica glass fibers is at a minimum.

4.2. Broadening of short light pulses

The upper bound of the transmission capability (data transmission rate, data bandwidth) of an optical fiber is determined by the minimum separation between neighboring data-coding pulses, which will not produce overlap and, consequently, symbol interference. There are three principal mechanisms that broaden short pulses propagating in optical fibers and thus restrict their bandwidth.

The broadening of a short light pulse propagating along a multimode fiber is due, above all, to the difference between the mode group velocities. In typical multimode optical fibers with core diameter of 50 μm and index difference between core and cladding of 0.01, there are several hundred propagating modes, and pulse broadening amounts to a few tens of nanoseconds per kilometer of fiber. This restricts the bandwidth to a few tens of MHz per kilometer of fiber length. The effect of the group velocity difference between modes can be sharply reduced by establishing a suitable index profile across the fiber (Fig. 1). A near-parabolic index profile will largely equalize the mode group velocities and will reduce the pulse broadening to something of the order of 0.1 ns/km. Graded-index optical fibers are now being manufactured with a bandwidth of more than 1 GHz·km (Ref. 23). We note that the above three methods of producing optical fibers can also be used to fabricate graded-index fibers.

The pulse broadening effect in step-index multimode fibers, and its reduction in graded-index fibers, can be graphically illustrated in terms of the ray approximation in which different modes correspond to rays propagating at different angles to the waveguide axis. Figure 8a shows ray propagation in a step-index multimode fiber, whereas Fig. 8b shows the situation in a graded-index fiber. It is clear that, in the former case, rays entering the waveguide at greater angles will traverse a longer path, and the radiation transported by them will arrive at the end of the fiber with a delay which produces pulse broadening. In the second case, rays entering the fiber at greater angles will also traverse a longer geometrical path, but some of this path lies in the region with the lower index, so that, provided the index profile is suitably chosen, the optical paths can be approximately equalized and thus substantially reduced the pulse broadening.

In optical fibers with the optimum index profile, and also in single-mode fibers, pulse broadening is largely due to chromatic dispersion, i.e., the fact that the refractive index of the fiber material is a function of wavelength. Since the optical pulse always has a finite spectral width, it will broaden even as it propagates in a single-mode fiber.

Pulse broadening due to chromatic dispersion in a fiber of length L is given by

$$\delta\tau = \frac{L}{c}\frac{d^2n}{d\lambda^2}\lambda\delta\lambda,$$

where c is the velocity of light in vacuum and $\delta\lambda$ is the spectral width of the radiation source. As an example, consider the broadening of a pulse produced by a GaAs light-emitting diode working at 800 nm with a spectral width of 16 nm. When this pulse propagates along the high-silica glass optical fiber, broadening by chromatic dispersion amounts to about 3 ns/km.

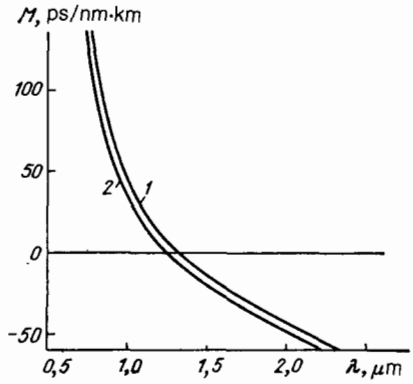

FIG. 9. Chromatic dispersion as a function of wavelength for high-silica glasses: $SiO_2 + GeO_2$ (1), SiO_2(2).

Pulse broadening due to chromatic dispersion is sharply reduced when the wavelength of incident radiation lies near 1.3 μm. Figure 9 shows the wavelength dependence[24] of chromatic dispersion, $M = \lambda / c \, d^2n/d\lambda^2$, of different high-silica glasses. It is clear that the chromatic dispersion of these glasses is zero near 1.3 μm. It is useful to note here that the region of negative chromatic dispersion of high-silica glass lies at wavelengths greater than 1.3 μm. This is important from the point of view of detection of certain nonlinear phenomena in optical fibers, which we shall consider in the next Section.

In the region close to zero chromatic dispersion, the pulse broadening is produced by waveguide dispersion, due to the dependence of the group velocity of a given mode on the geometry of the lightguide (in particular, the diameter of the core). Waveguide dispersion is usually small in comparison with chromatic dispersion across the entire spectral range, except for the region near the point of zero chromatic dispersion.

By suitably choosing the structure of the optical fiber, e.g., by using a multilayer structure, it is possible to annul chromatic dispersion by waveguide dispersion, since the two have opposite signs in the spectral range 1.3–1.4 μm. Signal distortion is then a minimum, and is determined by higher-order dispersion.[25,26] Estimates show that such single-mode fibers can transmit data at the rate of the order of a few hundred Gbit/s over a distance of 1 km.

We saw in the last Section that the optical loss of high-silica glass fibers is a minimum in the range 1.3–1.6 μm. Consequently, this is the most promising region for long-distance wide-band optical-fiber communication.[27]

4.3. Nonlinear optical phenomena in optical fibers

We have so far considered glass optical fibers, regarded as passive or linear media. Since the core material of glass fibers is isotropic, the first nonlinear term in the expansion of the polarization in terms of the field is the cubic term, i.e., the term representing the nonlinear polarization $P_n = \chi^{(3)}$ **EEE**. Despite the fact that the cubic nonlinearity in glass is small, the considerable length of optical fibers, their low optical loss, and their small transverse dimensions ensure that they are among the most interesting media for the observation of various nonlinear phenomena.

In fact, if we use an optical fiber of, say, 1 km or more, the length of the region of interaction between the laser radiation and the medium is increased by a factor of 10^5–10^6 as compared with the medium in bulk and comparable beam diameter. The core diameter of a single-mode fiber in the near infrared is 5–8 μm, so that when 1W of radiation is passed through the fiber, the power density is of the order of a few MW cm^{-2}.

The mode properties of optical fibers present us with new opportunities for investigating nonlinear phenomena. We have already seen that by varying the fiber parameters (core diameter and Δn) we can produce different propagation conditions for optical radiation, including single-mode, low-mode, low-mode with a given mode number, and multimode. Each mode has its own effective refractive index and an unvarying field configuration along the entire interaction length.

These properties enable us to use optical fibers to observe not only virtually all known nonlinear phenomena, but also many new and unique effects.

We are, in fact, facing the emergence of a new and rapidly developing branch of fiber optics, namely, nonlinear fiber optics.

We must now briefly consider some of the more interesting phenomena that also have important practical applications.

In high-silica glass, the Raman spectrum is wide and the vibrational frequency corresponding to the scattered intensity maximum lies at about 450 cm^{-1}. The first Stokes component of stimulated Raman scattering (SRS) is observed by using a pump of a few hundred mW. Cascade SRS can be produced relatively readily in a multimode fiber by using a Q-switched Nd-YAG laser ($\lambda = 1.06$ μm and 0.53 μm). The large number of Stokes components then covers the transparency range of high-silica glass up to 1.6 μm (Refs. 28-30). The high conversion efficiency (more than 50%) and relatively low process thresholds make this a very promising wide-band source of powerful radiation for different applications. It is also possible to produce tunable narrow-band SRS lasers either by laser pumping an optical fiber placed in a dispersive cavity,[31] or simply by inserting the fiber into the cavity of a garnet laser in which the crystal is pumped by a lamp.[32]

Stimulated Mandel'shtam-Brillouin scattering (SMBS) in optical fibers can be observed at even lower pump levels if the width of the pump spectrum is of the order of the line width of the Mandel'shtam-Brillouin scattering which for high-silica glass is of the order of 100 MHz. In the case of the argon laser pump, the minimum power level at which SMBS was observed in a 80-m single-mode fiber placed in the cavity was 15 mW (Ref. 33).
was 15 mW (Ref. 33).

Despite the fact that the SMBS gain in glass is greater than the SRS gain by more than two orders of magnitude, the latter process is usually the dominant one because the pump bandwidth is usually much greater than the Mandel'shtam-

Brillouin scattering line width.

SMBS in multimode optical fibers was investigated for the first time in Refs. 34 and 35. The multimode fibers were pumped by narrow-band laser radiation (Nd:YAG laser, $\lambda = 1.06\,\mu$m), and pump wavefront reversal was observed. The efficiency of nonlinear conversion of a pulse pump in SMBS ($\tau_p = 100$–300 ns) in a multimode fiber is very high, namely, more than 65%, and the threshold power is low (34 W; Ref. 34).

The specific features of nonlinear processes in optical fibers are clearly seen when four-photon mixing is investigated.[31] Stimulated four-photon processes are effective in laser-pumped optical fibers. In these processes, two pump photons (ν_p) create photons at the Stokes (ν_s) and anti-Stokes (ν_a) frequencies in accordance with the law of conservation of energy: $2\nu_p = \nu_s + \nu_a$. The phase-matching condition for the interacting waves is $2\mathbf{k}_p = \mathbf{k}_s + \mathbf{k}_a$ ($k_i = 2\pi n_i/\lambda_i$ where n_i is the refractive index). In bulk media with normal chromatic dispersion and collinear interaction between plane waves, we have $2\mathbf{k}_p < \mathbf{k}_s + \mathbf{k}_a$. Phase matching in such media is attained when waves interact at particular angles, and the interaction length is then small. In fiber lightguides, phase matching over a considerable length of the interaction region can be assured by compensating chromatic dispersion with intermode separation of pump waves and Stokes and anti-Stokes components into different modes with different effective refractive indices. Stimulated four-photon processes in low-mode fibers in which the phase matching conditions were satisfied were first observed when an optical fiber was pumped by a neodymium laser.[36] The frequency shifts $\Delta\nu = \nu_a - \nu_p = \nu_p - \nu_s$ were less than 400 cm^{-1}. Stimulated four-photon processes with frequency shifts of a few thousand cm^{-1} were observed later.[37,38] Frequency shifts up to $\Delta\nu = 5500\ \text{cm}^{-1}$ were reported in Ref. 37 for fiber lengths of a few meters and pump power ~ 1 kW. This can be used to produce by pumping with a neodymium laser generation in the region 1.4–1.6 μm, i.e., in the region of negative chromatic dispersion of high-silica glass.

There is undoubted interest in the investigation of four-photon processes in biharmonically-pumped optical fibers, which offer us new opportunities both for producing sources of narrow-band radiation that can be tuned over a wide range and for spectroscopic studies of the structure of phonon resonances in amorphous media.[39,40] In addition to the strong anti-Stokes wave at the frequency $\nu_a = 2\nu_1 - \nu_2$ ($\nu_1 > \nu_2$), which is formed in the low-mode fiber when the phase-matching conditions are satisfied, a strong Stokes wave was observed in Ref. 39 at the frequency $\nu_s = 2\nu_2 - \nu_1$ for which the intermode phase-matching condition need not be satisfied. Moreover, if the tuning range of the anti-Stokes wave is confined to a relatively narrow range by the phase-matching conditions, the tuning range of the Stokes wave is 1000 cm^{-1} or more.

The mechanism responsible for the above Stokes generation in biharmonically-pumped optical fibers without the phase-matching conditions being satisfied can be described as follows. A weak wave is created at the Stokes frequency $\nu_s = 2\nu_2 - \nu_1$ within the coherence length which for fused quartz is of the order of 1 cm. This wave is then exponentially amplified by stimulated Raman scattering in the pump field over a considerable length. The amplification of the wave ν_s occurs if the pump frequency difference is equal to the frequency of phonon resonances in the medium ($\nu_1 - \nu_2 = \nu_{ph}$). Actually, the measured dependence of the Stokes power on $\Delta\nu = \nu_1 - \nu_2$ is in reasonable agreement with the spontaneous Raman spectrum for fused quartz (Fig. 10).

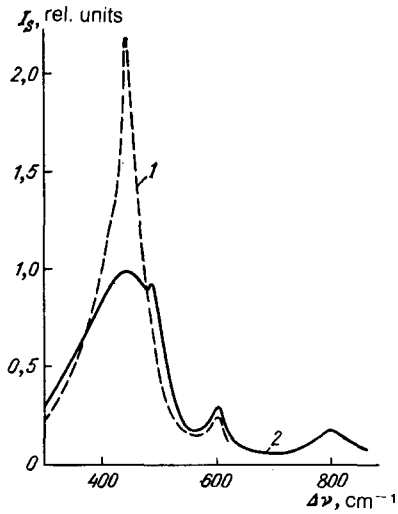

FIG. 10. Stokes-wave power at frequency $\nu_s = 2\nu_2 - \nu_1$ as a function of the frequency difference $\Delta\nu = \nu_1 - \nu_2$ (*1*), 2—spontaneous Raman scattering.

Nonlinear phenomena in glass optical fibers offer us new opportunities for picosecond and femtosecond pulse generation with controlled pulse parameters. It may be possible to exploit the nonlinearity of the refractive index of the fiber material to produce wide-range frequency scanning of the pulse field.[41,42] In contrast to the phase modulation of ordinary laser beams, the broadening of the spectrum in the homogeneous nonlinear medium of the single-mode optical fiber is not accompanied by a change in the spatial structure of the beam or energy redistribution over the cross section due to the accompanying nonlinear effects (self-focusing, nonlinear absorption, and so on). This results in a broadening of the laser pulse spectrum, which is uniform over the entire cross section.[43]

The combined effect of index nonlinearity and fiber dispersion produces the time-domain self-compression of pulses and gives rise to the appearance of optical envelope solitons in the region of negative group-velocity dispersion.

The propagation of the envelope of a light pulse is described by an equation called the parabolic or nonlinear Schrödinger equation:

$$i\left(\frac{\partial A}{\partial z}+\frac{1}{v_{gr}}\frac{\partial A}{\partial t}\right)=-\frac{1}{2}\frac{\partial^2 k}{\partial\omega^2}\frac{\partial^2 A}{\partial t^2}+\alpha K\frac{n_2}{n_0}|A|^2A,$$

where v_{gr} is the group velocity of the wave and α depends on the field distribution in the lightguide. When the loss δ must be taken into account, the term $-i\delta A$ must be added to the

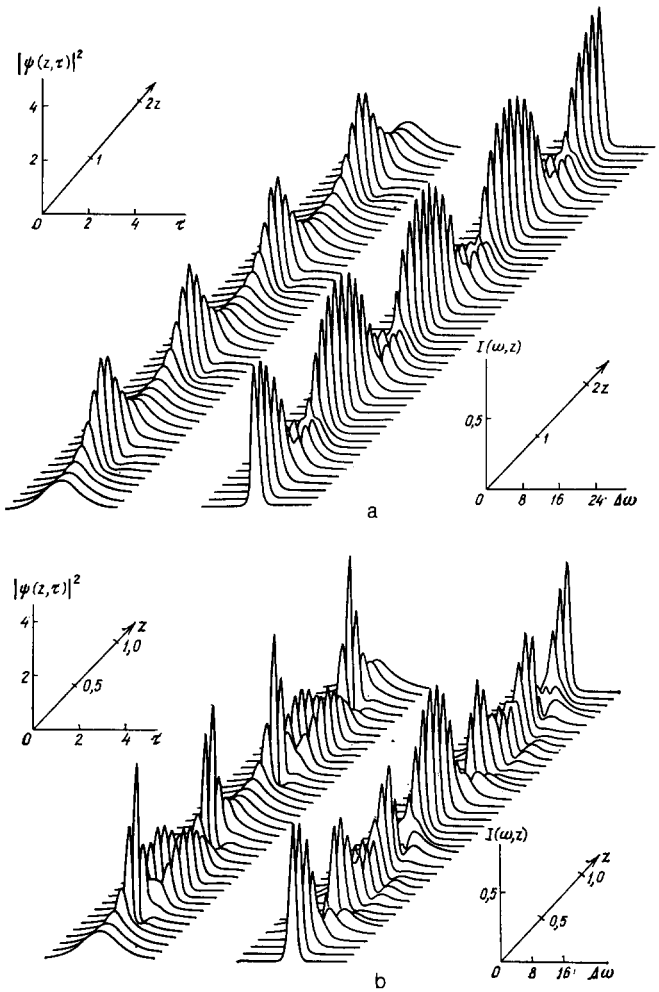

FIG. 11. Nonlinear dynamics of the time-domain envelope $|\psi(z,\tau)|^2$ and the spectrum $I(\omega, z)$ of 2- and 3- soliton pulses (a and b, respectively) in optical fibers. The variable z is normalized to the dispersion length and all other variables to their values at $z = 0$, $\tau = 0$, $\Delta\omega = 0$.

right-hand side of this equation. However, Zakharov and Shabat have shown that this equation has soliton solutions for the input pulse envelope in the form of the hyperbolic secant, the pulse amplitudes being multiples of the amplitude A_0 of the fundamental soliton.[44] The fundamental soliton does not change its shape during propagation, provided losses can be neglected. The second-order soliton has twice the amplitude, and the corresponding solution is periodic. The pulse contracts to its minimum width in half a period, and then expands again. Higher-order solitons have amplitudes that are multiples of A_0 and their behavior is more complicated. They not only contract, but also split (Fig. 11). In 1973, Hasegawa and Tappert predicted the possibility of solitons in optical fibers.[45] The soliton propagation of pulses in optical fibers made from high-silica glass was subsequently confirmed experimentally.[46]

The possibility of using soliton propagation of optical pulses in optical fibers as a means of data transmission has recently given rise to an extensive literature.[47–57] It has been shown [47,48,50,53–56] that the data transmission rate in the case of the soliton propagation of pulses in an optical fiber is restricted by the linear optical loss in the lightguide and the nonlinear interaction solitons.

Different ways of amplifying solitons and thus increasing the rate of data transmission along a lightguide have been proposed.[51,52,59] One of the most interesting ways of amplifying solitons in optical fibers is to exploit another nonlinear phenomenon, namely, stimulated Raman scattering.[52,57–59] It has been shown[59] that nonstationary stimulated Raman scattering in a low-mode optical fiber can be used not only to reconstruct the shape and energy of an optical pulse during its linear propagation along the fiber, but also to perform nonlinear soliton conversion.[57,58]

The use of high quality single-mode optical fibers as nonlinear phase modulators in dispersive compression of optical pulses has now given rise to considerable advances in ultrashort light pulse production. The method has been used to generated powerful picosecond pulses in the visible[60–62] and near infrared.[63,64] In particular, the compression of an initial 110-fs pulse was used in Ref. 60 to produce the shortest pulse duration so far, namely, 12 fs. The maximum compression (by a factor of 80) was reported in Ref. 61 where a 33-ps pulse was compressed. Spectral filtration was used in Ref. 65 to select picosecond pulses utilizing the combined effect of phase self-modulation and stimulated Raman scattering.

Light pulse compression can be performed directly in the optical fiber because of the negative group velocity dispersion of high-silica glass for $\lambda > 1.3\,\mu$m. This was used in Ref. 66 to achieve a 27-fold compression of 7-ps pulses at the wavelength of $1.55\,\mu$m, and a more than hundred-fold compression of 30-ps pulses[67,68] tunable in the range $1.5–1.6\,\mu$m. Efficient SRS conversion of such pulses resulted in single pedestal-free pulses of 200 fs and 56 kW (Ref. 68).

5. CONCLUSION

The main applications of fiber optics at present utilize optical fibers made from high-silica glass. The corresponding fiber technology is now good enough to produce commercial high-strength optical fibers with acceptable bandwidth and optical loss close to the theoretical limit. The minimum loss is about 0.2 dB/km in the near infrared. There have been rapid advances in fiber-optic communication. The most striking are the advances in the development of wideband optical-fiber communication lines. Suffice it to say that, in the last few years, optical data-transmission systems have been developed with transmission rates of a few Gbits/s over distances in excess of 100 km without the use of repeaters. The development of optical-fiber communication systems with heterodyne reception has increased the transmission range to a few hundred kilometers without the use of repeaters. Optical-fiber sensors will find extensive applications. Optical sensors of rotation, acoustic waves, temperature, magnetic field, ionizing radiation, and so on are under development.

However, for many applications, above all, for optical-fiber communications, it would be desirable to have optical fibers with still lower loss.

It is clear from Fig. 6 that the position and size of the fundamental loss minimum of glass is determined by two main mechanisms, namely, Rayleigh scattering (for which the scattered intensity falls off with wavelength as λ^{-4}) and the infrared absorption edge. If we were able to find materials in which the infrared lattice absorption tail could be shifted toward longer wavelengths, then the rapid decrease in Rayleigh intensity with increasing wavelength would ensure that the loss minimum would also shift toward longer wavelengths, and its size would decrease as well. A shift of the infrared lattice absorption edge toward longer wavelengths can be expected for materials consisting of heavier atoms. Calculations have actually shown that there are several materials (glasses and crystals) in which optical loss in the middle infrared range ($2 - 11\ \mu$m) can be 0.01–0.001 dB/km.

They include fluoride glasses with minimum optical loss in the range 3–4 μm (Ref. 69), chalcogenide glass with minimum loss at 5–6 μm (Refs. 70 and 71), and also crystals of the halogenides of metals with minimum loss at longer wavelengths.[72,73] The possibility of producing optical fibers with loss reduced by 1–2 orders of magnitude as compared with the high-silica glass has stimulated intensive research in this area.[74–77]

Fluoride and chalcogenide glasses with loss of the order 10 dB/km (Ref. 78) and a few tens of dB/km (Ref. 76), respectively, and polycrystalline fibers with loss of 100 dB/km at 10.6 μm (Ref. 79) have now been produced in the laboratory. Although this loss level exceeds by several orders the theoretical limit, the rapid advances made in this area suggest that a further rapid loss reduction will be achieved in infrared optical fibers.

The infrared optical fibers developed so far are promising for channeling powerful laser radiation (chemical, CO, and CO_2 lasers), for technological and medical applications, for temperature sensors, and for different location systems. The development of infrared lightguides with loss approaching the theoretical limit will result in optical-fiber communication lines with a transmission range of 1000 km without repeaters.

[1)]This paper is published in celebration of the 25th anniversary of the invention of the laser (1960) and continues the series of papers published in the January 1986 issue of this journal.

[1]K. C. Kao and G. A. Hockham, Proc. IEEE **133**, 1151 (1966).
[2]Zh. I. Alferov, V. M. Andreev, Yu. V. Garbuzov, Yu. V. Zhilyaev, E. P. Morozov, E. L. Portnoĭ, and V. G. Trofim, Fiz. Tekh. Poluprovodn. **4**, 1826 (1970) [Sov. Phys. Semicond. **4**, 1573 (1970)].
[3]A. H. Gnauck, B. L. Kasper, R. A. Linke, R. W. Dawson, T. L. Koch, T. J. Bridges, E. G. Burkhardt, R. T. Yan, D. P. Wilt, J. C. Campbell, K. Ciemiecki Nelson, and L. G. Cohen, in: Conference on Optical Fiber Communication, San Diego, California, 11-13 February 1985, PD2.
[4]T. G. Giallorenzi, Optics and Laser Techn., 1981, p. 73.
[5]"Advances in infrared fibers. II," Proc. SPIE, Los Angeles, 26-28 January 1981, 320.
[6]A. M. Prokhorov, Izv. Akad. Nauk SSSR Ser. Fiz. **47**, 1874 (1983) [Bull. Acad. Sci. USSR Phys. Ser. **47** (10), 1 (1983)].
[7]A. V. Belov, M. M. Bubnov, A. N. Gur'yanov, G. G. Devyatykh, E. M. Dianov, A. M. Prokhorov, S. Ya. Rusanov, and A. S. Yushin, Kvantovaya Elektron. (Moscow) **5**, 2064 (1978) [Sov. J. Quantum Electron. **8**, 1169 (1978)].
[8]D. Kalish, P. L. Key, C. R. Kurkjian, B. K. Tariyal, and T. T. Wang, in Optical Fiber Communication, ed. by S. E. Miller and A. G. Chynoweth, Academic Press, New York, San Francisco, London, 1979, p. 401.
[9]H. Schonhorn, C. R. Kurkjian, R. E. Jaeger, H. N. Vazirani, R. V. Albarino, and F. V. Di Marcello, Appl. Phys. Lett. **29**, 712 (1976).
[10]V. A. Bogatyrev, M. M. Bubnov, N. N. Vechkanov, A. N. Gur'yanova, E. M. Dianov, A. S. Konov, S. V. Lavrishchev, and A. Yu. Laptev, Kvantovaya Elektron. (Moscow) **9**, 1506 (1982) [Sov. J. Quantum Electron. **12**, 965 (1982)].
[11]Y. Tajima and S. Sakaguchi, Rev. Electr. Commun. Lab. **31**, 837 (1983).
[12]F. V. Di Marcello, D.L. Brownlow, R. C. Huff, and A. C. Hart, see Ref. 3, PD6.
[13]D. Marcuse, Optical Waveguides, Academic Press, 1974. [Russ. Trans., Mir, M., 1974].
[14]J. E. Midwinter, Optical Fibers for Transmission, John Wiley, 1979. [Russ. Trans., Radio i Svyaz', M., 1983].
[15]H. G. Unger, Planar Optical Waveguides and Fibers, OUP, 1977. [Russ. Transl., Mir, M., 1980].
[16]A. W. Snyder, IEEE Trans. Microwave Theor. Tech. **MTT-17**, 1310 (1961).
[17]D. Gloge, Appl. Opt. **10**, 2252 (1971).
[18]D. Gloge and E. A. J. Marcatili, Bell. Syst. Tech. J. **52**, 1563 (1973).
[19]T. Miyashita, T. Miya, and M. Nakahara, in: Topical Meeting on Optical Fiber Communication, Washington, 1979, PD-1.
[20]G. G. Devjatykh, N. H. Agliulov, and I. A. Zelyaev, in: Symposium über Halogenchemie, 4-6 April 1978, Berlin, GDR, p. 27.
[21]G. G. Devjatykh, N. H. Agliulov, V. L. Rodchenkov, V. A. Krylov, V. M. Vorotyntsev, A. E. Nikolaev, and E. M. Shcheplyagin, in: Fifth Intern. Symposium on High Purity Materials in Science and Technology, Dresedn, 5-9 May 1980, Poster-abstracts, p. 126.
[22]A. V. Belov, M. P. Braĭman, A. B. Grudinin, A. N. Gur'yanov, G. G. Devyatykh, E. M. Dianov, V. M. Il'in, V. M. Mashinskiĭ, V. B. Neustruev, A. M. Prokhorov, and V. F. Khopin, Kvantovaya Elektron. (Moscow) **11**, 646 (1984) [Sov. J. Quantum. Electron. **14**, 440 (1984)].
[23]M. Hoshikawa and K. Yano, in: Technical Digest of Fourth Intern. Conf. on Integrated Optics and Optical Fiber Communication, Tokyo, 1983.
[24]A. V. Belov, A. N. Gur'yanov, E. M. Dianov, V. M. Mashinskiĭ, V. B. Neustruev, A. V. Nikolaĭchik, and A. S. Yushin, Kvantovaya Elektron. (Moscow) **5**, 695 (1978) [Sov. J. Quantum Electron. **8**, 410 (1978)].
[25]A. S. Belanov, E. M. Dianov, and A. M. Prokhorov, *ibid.* **6**, 197 (1979) [**9**, 109 (1979)].
[26]A. S. Belyanov and E. M. Dianov, Radiotekhnika **37**, 35 (1982).
[27]E. M. Dianov, Kvantovaya Elektron. (Moscow) **7**, 453 (1980) [Sov. J. Quantum Electron. **10**, 259 (1980)].
[28]V. S. Butylkin, V. V. Grigor'yants, M. E. Zhabotinskiĭ, A. S. Petrosyan, and V. I. Smirnov. *ibid.* 621 [351].
[29]Z. V. Nesterova, I. V. Aleksandrov, I. V. Mel'nik, B. S. Neporent, D. K. Sattarov, and S. S. Safiulina, Pis'ma Zh. Tekh. Fiz. **6**, 661 (1980) [Sov. Tech. Phys. Lett. **6**, 286 (1980)].
[30]A. B. Grudinin, A. N. Gur'yanov, E. M. Dianov, E. A. Zakhidov, A. Ya. Karasik, and A. V. Luchnikov, Kvantovaya Elektron. (Moscow) **8**, 2383 (1981) [Sov. J. Quantum Electron. **11**, 1456 (1981)].
[31]R. H. Stolen, Fiber Integr. Optics **3**, 21 (1980).
[32]E. M. Dianov, S. K. Isaev, L. S. Kornienko, N. V. Kravtsov, and V. V. Firsov, Izv. Akad. Nauk SSSR Ser. Fiz. **43**, 266 (1979) [Bull. Acad. Sci. USSR Phys. Ser. **43**(2), 36 (1979)].
[33]D. Cotter, Electron. Lett. **18**, 495 (1982).
[34]T. T. Basiev, E. M. Dianov, and A. Ya. Karasik, A. V. Luchnikov, S. B. Mirov, and A. M. Prokhorov, Pis'ma Zh. Eksp. Teor. Fiz. **36**, 85 (1982) [JETP Lett. **36**, 104 (1982)].
[35]M. P. Petrov and E. A. Kuzin, Pis'ma Zh. Tekh. Fiz. **8**, 729 (1982) [Sov. Tech. Phys. Lett. **8**, 316 (1982)].
[36]R. H. Stolen, IEEE J. Quantum Electron. **QE-11**, 100 (1975).
[37]E. M. Dianov, E. A. Zakhidov, A. Ya. Karasik, P.V. Mamyshev, and A. M. Prokhorov, Zh. Eksp. Teor. Fiz. **83**, 39 (1982) [Sov. Phys. JETP **56**, 21 (1982)].
[38]C. Lin and M. A. Bösh, Appl. Phys. Lett. **38**, 479 (1981).
[39]T. T. Basiev, E. M. Dianov, E. A. Zakhidov, A. Ya. Karasik, S. B. Mirov, and A. M. Prokhorov, Pis'ma Zh. Eksp. Teor. Fiz. **37**, 192 (1983) [JETP Lett. **37**, 229 (1983)].
[40]T. T. Basiev, Yu. K. Voron'ko, E. M. Dianov, E. A. Zakhidov, P. G. Zverev, and A. Ya. Karasik, in: Abstracts of Papers presented at the Fourth All-Union Conf. on Laser Optics, State Optics Institute, Leningrad, 1983, p. 105.
[41]E. P. Ippen, C. V. Shank, and T. K. Gustafson, Appl. Phys. Lett. **24**, 190 (1974).
[42]V. N. Lugovoĭ, Pis'ma Zh. Eksp. Teor. Fiz. **22**, 416 (1975) [JETP Lett.

22, 200 (1975)].
[43]R. H. Stolen and C. Lin, Phys. Rev. Ser. A **17**, 1448 (1978).
[44]V. E. Zakharov and A. B. Shabat, Zh. Eksp. Teor. Fiz. **64**, 1627 (1973) [Sov. Phys. JETP **37**, 823 (1973)].
[45]A. Hasegawa and F. Tappert, Appl. Phys. Lett. **23**, 142
[46]L. F. Mollenauer, R. H. Stolen, and J. P. Gordon, Phys. Rev. Lett. **45**, 1095 (1980).
[47]A. Hasegawa and Y. Kodama. Proc. IEEE **69**, 1145 (1981).
[48]N. J. Doran and K. J. Blow, IEEE J. Quantum Electron. **QE-19**, 1883 (1983).
[49]I. N. Sisakyan and A. B. Shvartsburg, Kvantovaya Elektron. (Moscow) **11**, 1703 (1984) [Sov. J. Quantum Electron. **14**, 1146 (1984)].
[50]K. J. Blow and N. J. Doran, Electron. Lett. **19**, 429 (1983).
[51]A. Hasegawa and Y. Kodama, Opt. Lett. **7**, 285 (1983); **8**, 339.
[52]A. Hasegawa, Appl. Opt. **19**, 3302 (1984).
[53]E. M. Dianov, Z. S. Nikonova, and V. N. Serkin, Preprint IOFAN SSSR No. 13, Moscow, 1985.
[54]E. M. Dianov, A. M. Prokhorov, and V. N. Serkin, Dokl. Akad. Nauk SSSR **273**, 1112 (1983) [Sov. Phys. Dokl. **28**, 1036 (1983)].
[55]E. M. Dianov, Z. S. Nikonova, and V. N. Serkin, Kvantovaya Elektron. (Moscow) 1985 [*sic*].
[56]E. M. Dianov, A. M. Prokhorov, and V. N. Serkin, in: Technical Symposium on Infrared Optical Materials and Fibers, Proc. SPIE, Arlington, 3-4 May 1984, 484, p. 26.
[57]V. A. Vysloukh and V. N. Serkin, Pis'ma Zh. Eksp. Teor. Fiz. **38**, 170 (1983) [JETP Lett. **38**, 199 (1983)].
[58]V. A. Vysloukh and V. N. Serkin, Izv. Akad. Nauk SSSR Ser. Fiz. **48**, 1777 (1984) [Bull. Acad. Sci. USSR Phys. Ser. **48**(9), 125 (1984)].
[59]E. M. Dianov, Z. S. Nikonova, A. M. Prokhorov, and V. N. Serkin, Dokl. Akad. Nauk SSSR **283**, 1342 (1985); Preprint IOFAN SSSR No. 57, Moscow, 1985.
[60]J. M. Halbout and D. Grischkowsky, Appl. Phys. Lett. **45**, 1281 (1985).
[61]A. M. Johnson, R. H. Stolen, and W. M. Simpson, Appl. Phys. Lett. **44**, 729 (1984).
[62]S. A. Akhamnov, V. A. Vysloukh, L. Kh. Muradyan, S. M. Pershin, and A. A. Podshivalov, Preprint MGU No. 17, Moscow, 1984.
[63]E. M. Dianov, A. Ya. Karasik, P. V. Mamyshev, G. I. Onishchukov, A. M. Prokhorov, M. F. Stel'makh, and A. A. Fomichev, Kvantovaya Elektron. (Moscow) **11**, 1078 (1984) [Sov. J. Quantum Electron. **14**, 726 (1984)].
[64]J. D. Kafka, B. H. Kolner, T. Baer, and D. M. Bloom, Opt. Lett. **9**, 505 (1984).
[65]E. M. Dianov, A. Ya. Karasik, P. V. Mamyshev, G. I. Onishchukov, A. M. Prokhorov, M. F. Stel'makh, and A. A. Fomichev, Pis'ma Zh. Eksp. Teor. Fiz. **39**, 564 (1984) [JETP Lett. **39**, 691 (1984)].
[66]L. F. Mollenauer, R. H. Stolen, J. P. Gordon, and W. J. Tomlinson, Opt. Lett. **8**, 289 (1983).
[67]E. M. Dianov, A. Ya. Karasik, P. V. Mamyshev, G. I. Onishchukov, A. M. Prokhorov, M. F. Stel'makh, and A. A. Fomichev, Pis'ma Zh. Eksp. Teor. Fiz. **40**, 148 (1984) [JETP Lett. **40**, 903 (1984)].
[68]E. M. Dianov, A. Ya. Karasik, P. V. Mamyshev, A. M. Prokhorov, V. N. Serkin, M. F. Stel'makh, and A. A. Fomichev, *ibid.* **41**, 242 (1985) [**41**, 294 (1985)].
[69]S. Shibata, M. Horiguchi, K. Jinguji, S. Mitachi, T. Kanamori, and T. Manabe, Electron. Lett. **17**, 775 (1981).
[70]S. Shibata, Y. Terunuma, and T. Manabe, Jpn. J. Appl. Phys. **19**, 603 (1980).
[71]E. M. Dianov, M. Yu. Petrov, V. G. Plotnichenko, and V. K. Sysoev, Kvantovaya Elektron. (Moscow) **9**, 798 (1982) [Sov. J. Quantum Electron. **12**, 498 (1982)].
[72]A. L. Gentile, M. Braunstein, D. A. Pinnow *et al.*, in: Infrared Optical Materials in Fiber Optics: Advances in Research and Development, ed. by B. Bendow and S. Mitra, Plenum Press, New York, 1979, p. 105.
[73]E. M. Dianov, I. S. Lisitskiĭ, and V. G. Plotnichenko, Opt. Spektrosk. **55**, 1057 (1983) [*sic*].
[74]E. M. Dianov, see Ref. 5, p. 15.
[75]G. G. Devyatykh and E. M. Dianov, see Ref. 56, p. 105.
[76]T. Kanamori, Y. Terumuna, S. Takahashi, and T. Miyashita, Lightwave J. Tech. **LT-2**, 605 (1984).
[77]D. C. Tran, G. H. Sigel, and B. Bendow, *ibid.* 566.
[78]G. H. Sigel and D. C. Tran, see Ref. 56, p. 2.
[79]S. Kachi, K. Nakamura, M. Kimura, and K. Shiroyama, *ibid.* 128.

Translated by S. Chomet